Research Article

SCI

Received: 24 April 2014 Revised: 24 July 2014 Accepted article published: 4 August 2014 Published online in Wiley Online Library: 2 September 2014

(wileyonlinelibrary.com) DOI 10.1002/pi.4796

# Synthesis and thermal, mechanical and gas permeation properties of aromatic polyimides containing different linkage groups

**Ion Sava,[a*] Stefan Chisca,[a] Aleksandra Wolinska-Grabczyk,[b*] Andrzej Jankowski,[b] Mitica Sava,[a] Eugenia Grabiec[b] and Maria Bruma[a]**

## Abstract

**Two series of aromatic polyimides containing various linkage groups based on 2,7-bis(4-aminophenoxy)naphthalene or 3,3′-dimethyl-4,4′-diaminodiphenylmethane and different aromatic dianhydrides, namely 4,4′-(4,4′-isopropylidenediphenoxy) bis(phthalic anhydride), 4,4′-(hexafluoroisopropylidene)bis(phthalic anhydride), 3,3′,4,4′ benzophenonetetracarboxylic dianhydride, 9,9-bis[4-(3,4-dicarboxyphenoxy)phenyl]fluorene dianhydride and 4,4′-(4,4′-hexafluoroisopropylidenediphenoxy)bis (phthalic anhydride), were synthesized and compared with regard to their thermal, mechanical and gas permeation properties. All these polymers showed high thermal stability with initial decomposition temperature in the range 475–525 °C and glass transition temperature between 208 and 286 °C. Also, the polymer films presented good mechanical characteristics with tensile strength in the range 60–91 MPa and storage modulus in the range 1700–2375 MPa. The macromolecular chain packing induced by dianhydride and diamine segments was investigated by examining gas permeation through the polymer films. The relationships between chain mobility and interchain distance and the obtained values for gas permeability are discussed.**


**Keywords:** polyimides; thin films; thermal properties; gas permeation; morphology

## INTRODUCTION

Aromatic polyimides are one of the most heat-resistant classes of polymers and are widely used in high-temperature plastics, adhesives, dielectrics, photoresists, membrane materials for gas separation and Langmuir–Blodgett films.[1–6] Thus, polyimides are very attractive for large-scale industrial applications, such as aerospace, defence and optoelectronics, owing to their exceptional chemical, physical and thermal stability, mechanical robustness and structural diversity.[1,6,7] However, wholly aromatic polyimides are processed with great difficulty because they are insoluble and infusible, and do not show any glass transition before decomposition due to their aromaticity that induces rigidity and strong intermolecular interactions.[8–11]

Therefore, much research is carried out on new polyimides, which should be soluble in certain solvents and could be processed by using solutions of the already cyclized polyimides. There are some approaches generally implemented in order to improve polyimide solubility: incorporation of flexible or non-symmetric linkages into the backbone, introduction of large pendant substituents or 'kinks' to the polymer chain, or disruption of symmetry and recurrence of regularity through copolymerization. For instance, the incorporation of flexible linkages, such as -O-, -$CH_2$-, -$SO_2$- and hexafluoroisopropylidene groups, into the polyimide backbone decreases the rigidity of the polymer chain, whereas introduction of bulky pendant groups disrupts chain packing efficiency. Both factors reduce the interchain interactions and lead to enhanced solubility without sacrificing the high thermal stability.[12–16]

Aromatic polyimides are also promising materials for gas separation applications.[6] They exhibit a combination of high permeability and selectivity along with other desirable properties important from a membrane manufacturing point of view. Moreover, their gas separation properties can be largely modified to meet the demands of a particular separation process by appropriate adjustment of chemical structures in a polymer chain.[17,18] Generally, to improve gas transport properties, an approach of introducing solubilizing moieties into the polymer chain can be used. An increased permeability can be achieved by hindered chain packing, while improved selectivity can be achieved by reduced rotational mobility around flexible linkages in the polymer backbone. This strategy to produce soluble and permeable polyimides is very often based on the introduction of bulky moieties into the main chain. There are examples in the literature of polyimide structure optimization using this guideline, e.g. of introducing two bulky groups into the central ring of an *m*-terphenyl moiety[19] and of incorporating diphenylfluorene

* *Correspondence to: Ion Sava, 'Petru Poni' Institute of Macromolecular Chemistry, Aleea Grigore Ghica Voda 41A, Iasi, Romania. E-mail: isava@icmpp.ro or Aleksandra Wolinska-Grabczyk, Centre of Polymer and Carbon Materials, Polish Academy of Sciences, 41-819 Zabrze, M. Curie-Sklodowska Str 34, Poland. E-mail: awolinska@cmpw-pan.edu.pl*

*Paper dedicated to the 65th anniversary of 'Petru Poni' Institute of Macromolecular Chemistry of the Romanian Academy, Iasi, Romania*

a *'Petru Poni' Institute of Macromolecular Chemistry, Aleea Grigore Ghica Voda 41A, Iasi, Romania*

b *Centre of Polymer and Carbon Materials, Polish Academy of Sciences, 41-819 Zabrze, M. Curie-Sklodowska Str 34, Poland*

 

moiety[20] or adamantyl ester pendant groups[21] in the main chain. Another approach reported in the literature is based on incorporation of monomers having internal free volume.[22] Recently, the concept of introducing spiro-centres into a polyimide main chain has attracted much attention.[23–26] Additionally, an interesting route of using soluble hydroxyl-substituted polyimides as precursors of insoluble poly(benzoxazole)s has been demonstrated.[27,28] These new groups of polyimide-based membrane materials have been shown to have attractive gas transport properties with permeability and selectivity values very often near to or above the Robeson upper bound.[29] Although there are numerous studies in the literature reporting polyimides synthesized using different combinations of diamine and dianhydride reagents, research on structure–property relationships allowing for further material development is still needed.

In this paper we report a comparative study of two series of polyimides obtained from polycondensation reaction of aromatic diamines containing ether linkages, namely 2,7-bis(4-aminophenoxy)naphthalene (BAPN) or 3,3′-dimethyl-4,4′-diaminodiphenylmethane (MMDA), with different dianhydrides containing flexible and/or bulky ether, isopropylidene, hexafluoroisopropylidene and fluorene units. The inclusion of flexible linkages and bulky groups together with a rigid aromatic unit, such as naphthalene, in the same chain was expected to render polyimides with both good solubility and processability, and still good thermal stability. The introduction of bulky substituents into the main chain should also lead to an increase of free volume and to enhanced permeability through the polyimide films. Additionally, the selection of BAPN instead of 2,6-bis(4-aminophenoxy)naphthalene reported in the literature[30] was supposed to further improve polyimide solubility while maintaining good thermal stability. The polyimides synthesized from BAPN are new. The MMDA-based polyimides reported here were studied by us previously with respect to their dielectric behavior.[31] The polyimide from hexafluoroisopropylidene-bis(phthalic anhydride) and MMDA has also been investigated by Han *et al.* who reported its excellent properties as a candidate material for the fabrication of porous polymer films with ordered structure.[32] In the present work, MMDA-based polyimides were examined with respect to their gas permeation properties and optical transparency. However, some additional characterization was also performed to obtain data complementary to those resulting from the extensive analysis of the BAPN-based series. It was believed that both data sets would enable us to get a better understanding of the respective structure–property relationships required for the development of high-performance polyimides.

## EXPERIMENTAL

### Materials

The two aromatic diamines used in this study, namely BAPN (**Ia**) and MMDA (**Ib**), were obtained in our laboratory using previously reported methods.[33,34] The melting point (m.p.) of BAPN was 172–175 °C and that of MMDA was 155–157 °C.

4,4′-(4,4′-Isopropylidenediphenoxy)bis(phthalic anhydride) (**IIa**), 4,4′-(hexafluoroisopropylidene)bis(phthalic anhydride) (**IIb**) and 3,3′,4,4′-benzophenonetetracarboxylic dianhydride (**IId**) were purchased from Aldrich, and were purified in our laboratory by recrystallization from acetic anhydride. The m.p. of **IIa** was 184–187 °C, m.p. of **IIb** was 245–247 °C and m.p. of **IId** was 224–226 °C.

9,9-Bis[4-(3,4-dicarboxyphenoxy)phenyl]fluorene dianhydride (**IIc**) and 4,4′-(4,4′-hexafluoroisopropylidenediphenoxy)bis(phthalic anhydride) (**IIe**) were obtained in our laboratory by previously reported methods.[35,36] The m.p. of **IIc** was 239–241 °C and m.p. of **IIe** was 232–234 °C. *N*,*N*′-dimethylacetamide (DMAc; Merck) was used as received.

### Synthesis of polymers

The investigated polyimides (**PI-1–PI-8**) were obtained by a two-step polycondensation reaction.[37] The first step was performed at room temperature with equimolar amounts of aromatic diamines and dianhydrides in DMAc at a total concentration of 12–15%, under inert atmosphere during 6–7 h (Scheme 1).

In the second step, thermal imidization of the resulting poly(amic acid) in solution was performed in the same reaction flask by heating the solution at reflux temperature (170–180 °C) for 5–6 h, under a slow stream of nitrogen to remove the water of imidization. The final product was precipitated in water, washed with water and ethanol, and dried in a vacuum oven at 105 °C.

The polyimide films were obtained by casting the respective polyimide solution in DMAc onto a glass plate and by drying at 60 °C for 4 h. Then the films were further dried at 100, 150, 200 and 250 °C for 1 h at each temperature. Finally, the films were kept at 260 °C for 4 h and they were used afterwards for various measurements. The thickness of such films was in the range 30–40 μm. The film from **PI-4**, due to the polymer precipitating during thermal imidization, was obtained from poly(amic acid) followed by high-temperature imidization in the already formed film. The structures and the abbreviations of the polyimides are listed in Table 1.

### Measurements

Fourier transform infrared (FTIR) spectra were recorded with a FTIR VERTEX 70 (Bruker Optics Company), with a resolution of 0.5 $cm^{-1}$. $^1H$ NMR spectra were recorded with a Bruker Avance DRX 400 spectrometer in deuterated chloroform ($CDCl_3$) or dimethylsulfoxide (DMSO-$d_6$) solution.

Weight-average ($M_w$) and number-average ($M_n$) molecular weights were determined by means of gel permeation chromatography (GPC) using a Waters GPC apparatus, provided with refraction and photodiode array detectors and a Phenomenex-Phenogel MXN column. Measurements were carried out with polymer solutions of 0.2% concentration, using *N*,*N*-dimethylformamide (DMF) as eluent. Polystyrene standards of known molecular weight were used for calibration.

Optical transmission measurements were performed with a JASCO V570 UV–vis-NIR spectrophotometer within the range 200–2500 nm. Standard ATSM test method for yellowness index (YI) of plastics and polymer materials, D1925-70 (reapproved 1988), was used for the determination of the YI values.

AFM measurements were performed in air, at room temperature (23 °C), in tapping mode using a scanning probe microscope (Solver PRO-M, NT-MDT, Russia) with commercially available NSG10/Au cantilevers with a nominal elasticity constant $K_N = 11.5$ N $m^{-1}$.

The tensile properties were recorded with a Shimadzu AGS-J deformation apparatus at ambient temperature and at a rate of deformation of 1 mm $min^{-1}$ with a load cell capable of measuring forces up to 1 kN. For each data point, five film samples of 20 mm × 5 mm were tested and the average value was taken.

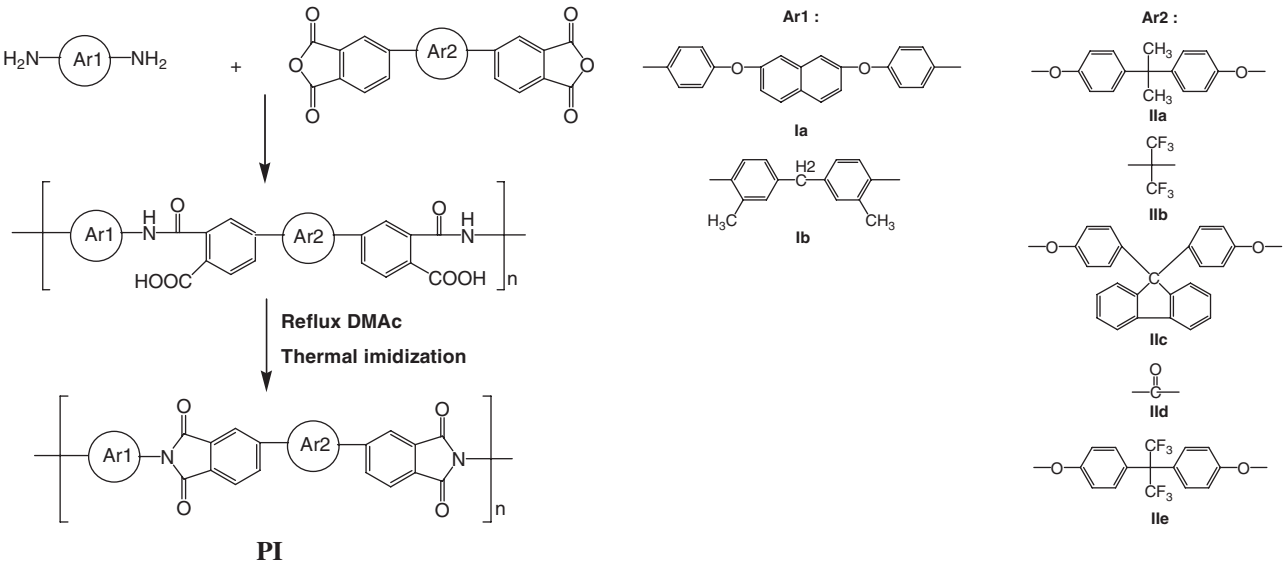


**Scheme 1.** Synthesis of the investigated polyimides.

XRD patterns of film samples were recorded using Cu K$\alpha$ radiation (wavelength $\lambda = 1.54051$ Å) with a wide-angle HZG-4 diffractometer (Carl Zeiss, Jena, Germany) working in the typical Bragg geometry. The XRD angle, $\Theta$, at which the maximum of a broad peak appeared in the wide-angle XRD profile and the Bragg equation

$$\lambda = 2d \sin \Theta \tag{1}$$

were used for calculation of an average interchain distance, the *d*-spacing.

DSC experiments were performed with a TA-DSC 2010 apparatus (TA Instruments, Newcastle, DE, USA) under nitrogen using a heating/cooling rate of 20 °C min$^{-1}$. The glass transition temperature, $T_g$, was taken as the midpoint of the heat capacity step change observed during the second run. TGA was carried out by using a Q-1500-D thermobalance (Budapest, Hungary), in the temperature range 25–800 °C, at a heating rate of 10 °C min$^{-1}$, under controlled flux of nitrogen.

Permeation measurements were made at 7 bar (0.7 MPa) of applied gas pressure, and at 30 °C using a constant-pressure/variable-volume apparatus.[38] Pure helium, oxygen, nitrogen and carbon dioxide were used for permeation experiments, and those gases were measured in the given sequence. The gas permeability, *P*, expressed in Barrer units, was determined according to the equation

$$P = \frac{ql}{(p_1 - p_2)\,At} \tag{2}$$

where *q* is the quantity of a permeant (cm$^3$ (STP)) passing through the membrane in time *t* (s), *A* is the effective membrane area (cm$^2$), *l* is the membrane thickness and $p_1$ and $p_2$ are the upstream and downstream pressures, respectively. The error of the permeability coefficient associated with this system was determined to be 10–15%, the error being larger the lower the gas permeability. From single gas permeation experiments, and using the following equation, the ideal selectivity ($\alpha$) for gases A and B was also calculated:

$$\alpha = \frac{P_A}{P_B} \tag{3}$$

## RESULTS AND DISCUSSION

### Basic characterization of polyimide films

The imide structure of the polymers was identified from their FTIR spectra. In Fig. 1, representative FTIR spectra of **PI-2** and **PI-8** are shown. The presence of absorption bands for carbonyl group of the imide ring at about 1770–1780 and 1710–1720 cm$^{-1}$, and characteristic bands for C-N vibration at 1370–1375 and 720–730 cm$^{-1}$ indicate the formation of imide rings.[39,40] All polyimides show characteristic absorption bands for C=C aromatic vibration around 3060 and 1600 cm$^{-1}$.

The presence of ether linkages (C-O-C) is evidenced from bands at 1215–1240 cm$^{-1}$. These characteristic absorption bands are overlapping with those of imide $(CO)_2$ N bands.[39] Additional bands at 2850–2920 cm$^{-1}$ observed for polymers **PI-1**, **PI-6**, **PI-7** and **PI-8** are attributed to characteristic absorption of methyl and methylene units. No absorption is seen in the range 3350–3400 cm$^{-1}$, which is usually present in the spectra of non-cyclized poly(amic acid) precursors.

$^1$H NMR spectra of the synthesized polyimides were recorded in order to confirm the structure of the polymers. Spectra of representative examples of each series of polyimides are shown in Fig. 2.

In the aromatic region, polyimide **PI-2** exhibits distinct multiplets due to the aromatic protons of phenylene, naphthalene and phthalimide rings, as follows: 8.02–8.04 ppm (2H, d), 7.92 ppm (2H, s), 7.83–7.88 ppm (4H, m), 7.37–7.40 ppm (4H, d), 7.32 ppm (2H, s), 7.21–7.23 ppm (2H, d) and 7.16–7.18 ppm (4H, d). The $^1$H NMR spectrum of polyimide **PI-8** shows various multiplets in the aromatic region due to the aromatic protons from benzophenone and diamine structure, as follows: 8.1–8.3 ppm (6H, m), 7.32–7.35 ppm (2H,d), 7.26–7.28 ppm (2H,d) and 7.21 ppm (2H,s). Also, in the aliphatic region characteristic signals of -$CH_3$ and -$CH_2$- groups of the diamine segment are present at around 4 ppm (2H,s) and 2.1 ppm (6H,s). The complete cyclization of all poly(amic acid)s is confirmed by the absence of the characteristic signals of protons from carboxyl and amidic groups in the range 9–14 ppm.

Except for **PI-4**, all polyimides are easily soluble in the following solvents: *N*-methyl-2-pyrrolidone (NMP), DMAc, DMF, DMSO, chloroform ($CHCl_3$) and tetrahydrofuran (THF). The good solubility is



  

**Table 1.** Structures and the abbreviations of the polyimides

| Polymer | Monomer: Diamine | Monomer: Dianhydride |
|---|---|---|
| | $H_2N$–Ar1–$NH_2$ | Ar2 |
| | Ar1 | Ar2 |
| **PI-1** | 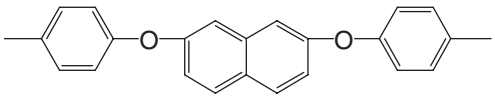 | 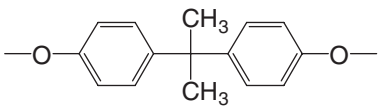 |
| **PI-2** | 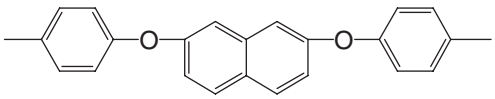 | 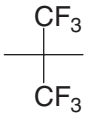 |
| **PI-3** | 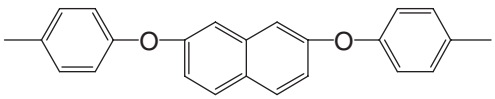 | 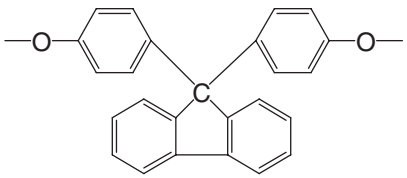 |
| **PI-4** | 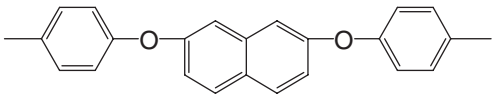 |  |
| **PI-5** | 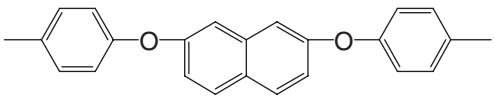 | 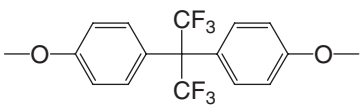 |
| **PI-6** | 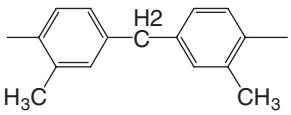 | 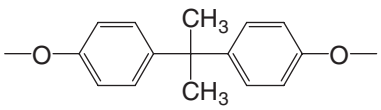 |
| **PI-7** | 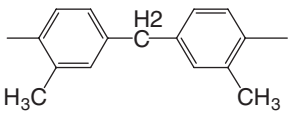 | 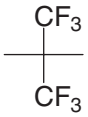 |
| **PI-8** | 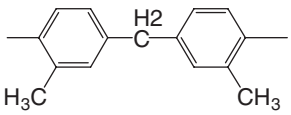 |  |

apparently due to the effects of flexible bridges in the diamine segments, such as ether or methylene groups, and to the presence of isopropylidene, hexafluoroisopropylidene or fluorene units from the dianhydride segments, which increase the free volume allowing for the small solvent molecules to penetrate more easily among the polymer chains. The steric hindrance of these bulky groups might also lead to a distortion of the packing of the polyimide backbones. The incorporation of all these segments into the polyimide chains leads to a decrease of the molecular packing and as a consequence to increased solubility. Also, it is proved that the presence of 2,7-BAPN instead of 2,6-BAPN improves polyimide solubility. Comparing the solubility of **PI-2** synthesized in this work with that reported in literature for the corresponding polyimide obtained using 2,6-BAPN,[30] it appears that the latter is soluble in NMP, DMAc and DMF only on heating, and insoluble in DMSO and THF, whereas **PI-2** is easily soluble in all these solvents.

In Table 2, the inherent viscosities of the polyimides and the values of their molecular weights and polydispersities ($M_w/M_n$) are listed. The inherent viscosity values are in the

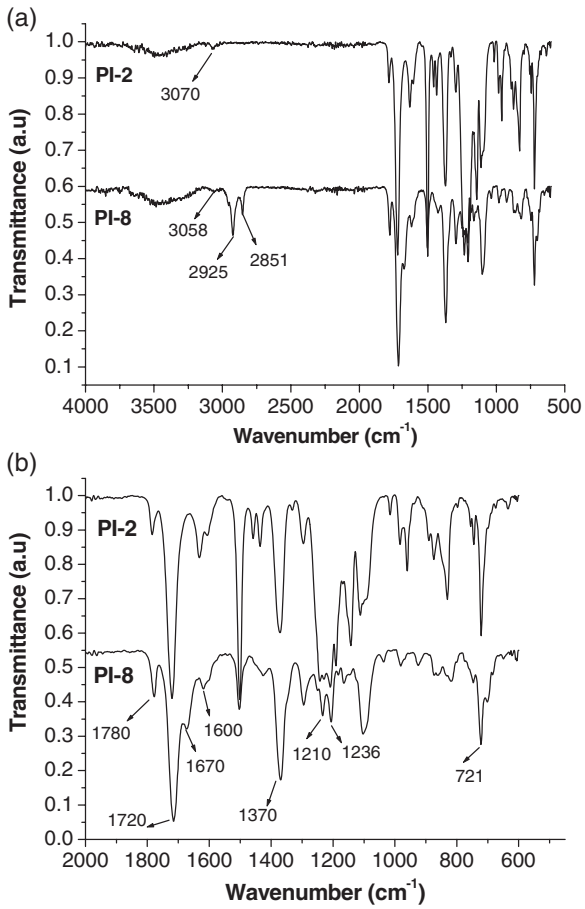


**Figure 1.** FTIR spectra of **PI-2** and **PI-8**: (a) in the range 4000–500 $cm^{-1}$; (b) in the range 2000–500 $cm^{-1}$.

range 0.3–0.46 dL $g^{-1}$ indicating the versatile solubility of these polymers that allows for easy solution processing. The GPC measurements give the following molecular weight data: $M_w$ in the range 40 000–62 000 g $mol^{-1}$, $M_n$ in the range 21 000–28 000 g $mol^{-1}$ and $M_w/M_n$ values around 2 that are typical for polycondensation reactions. However, these values have to be taken as indicative only, since calibration with polystyrene standards may result in questionable results as the polarity and backbone stiffness of the studied polymers deviate strongly from those of polystyrene.

The synthesized polyimides gave flexible and free-standing films on casting from polymer solutions or, in the case of **PI-4**, from its non-cyclized poly(amic acid) precursor. All of the PI films are yellow, typical for aromatic polyimides, and optically transparent. The UV-visible spectra of the films with thicknesses of 30–40 μm are shown in Fig. 3. Within the transparency spectral range, the transmission of the films studied reached values of 80–90%. The YI values calculated from the spectra and listed in Table 2 are in the range 24–94. Polymers **PI-4** and **PI-8**, both produced from BTDA, exhibit the highest YI values, 94 and 72, respectively, and they have deeper colour than the other polyimides. A similar observation concerning higher colour intensity than that expected has already been reported in literature for other **IId**-based polyimides.[41] Comparing the optical transparency of the remaining polyimides, it can be noticed that some of them have YI values of 24 to 33, which are relatively low for fully aromatic polyimides. It is generally accepted that interactions between the alternating electron-donor and electron-acceptor moieties, introduced by diamine and dianhydride monomers into a polymer chain, lead to the formation of charge transfer complexes (CTC), which are responsible for the coloration of aromatic polyimides.[42] The better optical transparency of some polyimides is usually attributed to the suppressed formation of CTCs being a result of disrupted chain packing.[43,44] For the polyimides under investigation, the low YI values for some of them can be associated with the presence of hexafluoroisopropylidene, isopropylidene or fluorene groups preventing CTC formation through steric hindrance.

Figure 4 shows XRD patterns of the studied polyimide films. These wide-angle XRD patterns exhibit a single broad diffraction peak which is typical for amorphous polymers. The distance associated with the peaks of the polyimides is found to be in the range from 4.35 to 5.75 Å (Table 3). This means that the applied structural variations give rise to widely varied *d*-spacing values. This effect is particularly noticeable for the BAPN-based series of polyimides containing naphthalene units, where the impact of the unit from the dianhydride monomer is not obscured by that resulting from the presence of other sterically bulky groups like methyl-substituted diphenylmethane unit of MMDA. Thus, placement of a sterically small carbonyl connector between phthalimide rings gives a polymer with the lowest *d*-spacing value. On the other hand, introduction of increasingly bulkier groups, diphenylfluorene (**PI-3**), isopropylidene (**PI-1**) and particularly hexafluoroisopropylidene (**PI-5** and **PI-2**), increases the interchain distance, as has been reported in the literature.[45–47] The same trend of increasing interchain distance can be observed for the polyimide series based on MMDA. The respective *d*-spacing values of these polymers are found to be higher than those determined for the series of polyimides based on BAPN. This is likely to be due to a decrease in packing efficiency resulting from methyl substitution at the 3,3′-positions of the MMDA aromatic rings. However, the influence of bulky and sterically hindered hexafluoroisopropylidene linkages appears to be dominant, and *d*-spacing values for **PI-2** and **PI-7** are comparable, 5.68 and 5.75 Å, respectively.

## Thermal properties of polyimide films

Thermal behaviour of the synthesized polyimides was investigated using TGA and DSC. Representative DSC curves for the first and second heating runs of **PI-2** are shown in Fig. 5. On the first heating run, endotherms are observed which accompany the stepwise change of the specific heat of the polyimide at the glass transition. Most likely these peaks can be related to stress release.

Since all the polyimides have the same thermal history, this seems to indicate that the amount of the stress release is the largest for the most rigid structures of **PI-2** and **PI-7**. Comparing **PI-2** and **PI-5**, having the same **IIb** structural unit, it can be noticed that **PI-5** containing additional ether linkages, which enhance chain mobility, shows a much smaller endotherm ($\Delta H = 0.44$ J $g^{-1}$) than that of polymer **PI-2** ($\Delta H = 1.4$ J $g^{-1}$). Comparing the first and second heating DSC scans, a small shift towards higher temperatures at the beginning of the glass transition is observed.

The values of $T_g$ taken from the second heating scan are listed in Table 3. These data show that the $T_g$ values vary considerably with the molecular structure of the polymers. The polyimides synthesized from BAPN, which contains two ether bridges, exhibit lower $T_g$ than the related ones obtained from the same dianhydride but with MMDA, which does not have any ether



  

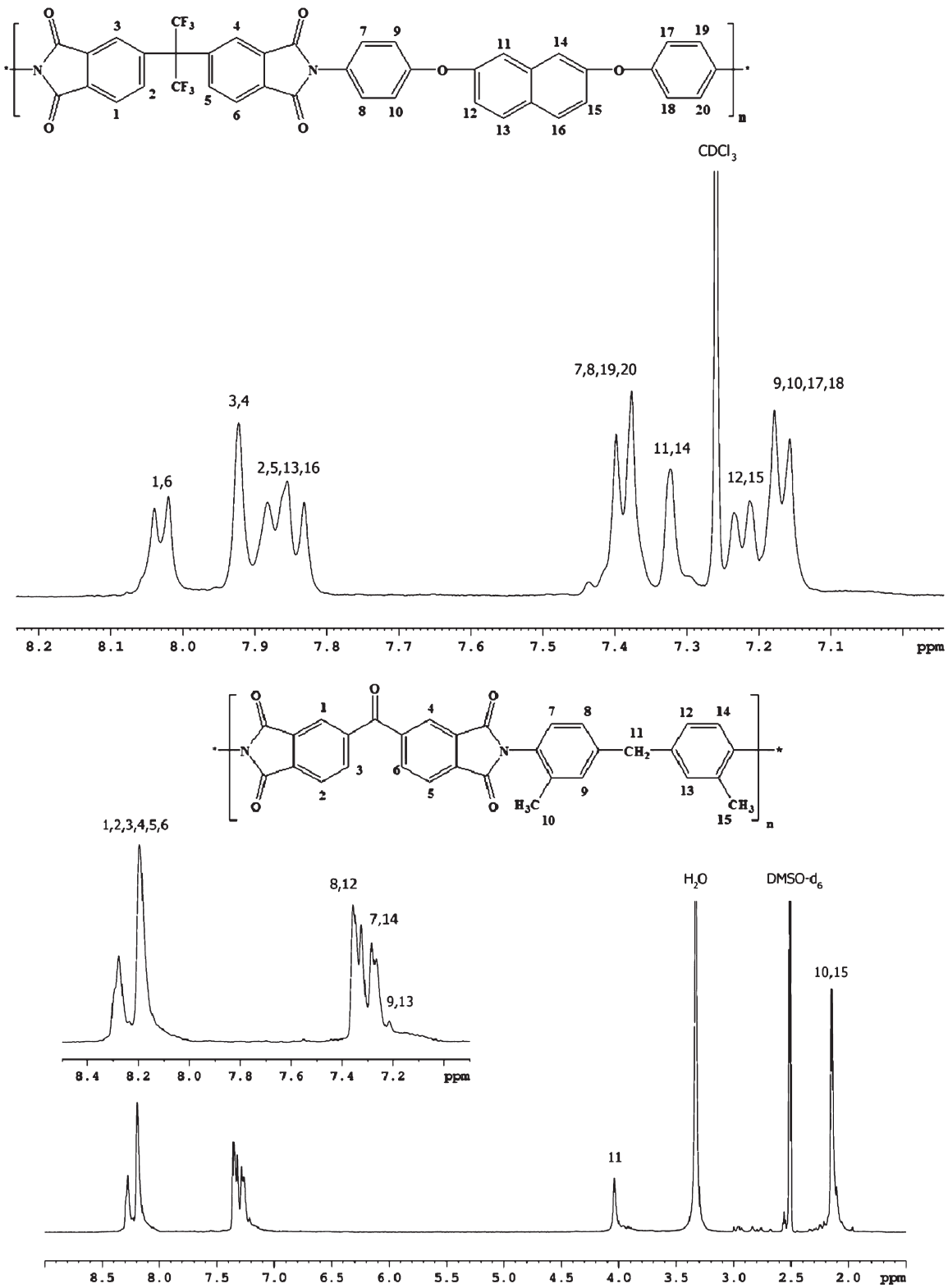


**Figure 2.** $^{1}$H NMR spectra of polyimides **PI-2** and **PI-8**.

bridges. The observed difference is around 20 °C for the corresponding polyimides indicating that ether bonds enhance chain mobility effectively. This is also illustrated by the $T_g$ data for **PI-2** and **PI-5** where the effect of ether groups is even more pronounced, and where a reduction in $T_g$ of 53 °C can be observed. Accordingly, the lowest $T_g$ value is obtained for **PI-1** due to the largest amount of ether linkages and to the presence of methyl groups instead of $CF_3$ ones (**PI-5**), which are less bulky and not so effective in hindering the intra-segmental mobility. On the other hand, introduction of a rigid aromatic structure

**Table 2.** Inherent viscosities, molecular weights and yellowness index (YI) values of polyimides

| Polymer | Inherent viscosity[a] (dL g$^{-1}$) | $M_w$ (g mol$^{-1}$) | $M_n$ (g mol$^{-1}$) | $M_w/M_n$ | YI |
|---|---|---|---|---|---|
| **PI-1** | 0.30 | 40 000 | 22 000 | 1.82 | 27 |
| **PI-2** | 0.33 | 62 000 | 27 000 | 2.30 | 28 |
| **PI-3** | 0.31 | 46 000 | 23 500 | 1.96 | 24 |
| **PI-4** | _ [b] | _ [b] | _ [b] | _ [b] | 94 |
| **PI-5** | 0.38 | 59 000 | 28 000 | 2.11 | 59 |
| **PI-6** | 0.46 | 54 000 | 28 000 | 1.93 | 33 |
| **PI-7** | 0.40 | 42 500 | 21 000 | 2.02 | 49 |
| **PI-8** | 0.44 | 52 000 | 25 000 | 2.08 | 72 |

[a] Measured for polymer solutions in NMP, at 0.5 g dL$^{-1}$ concentration and at 20 °C.
[b] Insoluble.

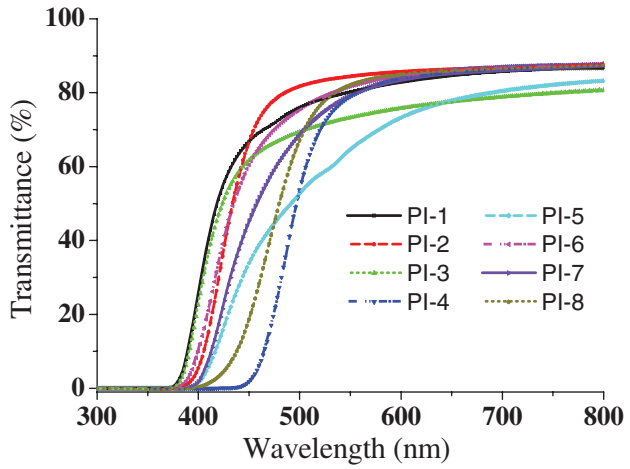


**Figure 3.** UV-visible spectra of the polyimide films

with a $C(CF_3)_2$ connector (**PI-2** and **PI-7**) leads to a noticeable increase in $T_g$. Thus, **PI-7**, based on MMDA, shows the highest $T_g$ value among the polymers studied. The influence of the structural units on polyimide main chain mobility found for the polyimides studied is in good accordance with observations made by us previously,[31,48] and with other results presented in the literature.[20,30,32,49,50]

The TGA results for the studied polyimides are shown in Fig. 6, and the corresponding data are listed in Table 3. It can be seen that BAPN-based polyimides show higher thermal stability than MMDA-based ones, with temperature of 5% weight loss being in the ranges 505–525 °C and 475–498 °C, respectively.

Thus, polyimides based on BAPN start to degrade at temperatures higher by approximately 25 °C than MMDA-based polyimides. Among the polymers investigated, **PI-6** with four methyl groups per repeat unit shows the lowest thermal stability. The temperature corresponding to 5% weight loss of **PI-6** is 475 °C, whereas that of **PI-1**, which is also prepared from **IIb** but contains only two methyl substituents, is 505 °C. **PI-1** is the least stable polymer within the BAPN-based series of polyimides. Similarly, the temperature of maximum degradation rate has the lowest value (515 °C) for **PI-6**, while the values for the other polyimides are in the range 540–580 °C. It should be pointed out that **PI-2**, **PI-5** and **PI-7**, all having $CF_3$ substituents in their chains, show a shoulder in their degradation curves. This shoulder appears at higher temperature, above 610 °C, depending on polyimide structure, and the experimental weight loss at this step is around 6%, much smaller than that during the first major step. Since C-F bonds are generally more stable than C-H ones, the effect observed in this temperature range is probably connected with degradation involving chain fragments with $CF_3$ substituents. Taking into account the char yield at 800 °C, it can be noticed that the investigated polyimides show a high amount of residual weight, being in the range 60–66% for all polyimides.

## Mechanical properties and surface morphology of polyimide films

Table 4 presents some mechanical properties, namely tensile strength, elongation at break and Young's modulus, of the polyimide films. The values of tensile strength and elongation at break are in the ranges 64–91 MPa and 4.1–8.8%, respectively, and they are comparable with the values obtained for other polyimides or for polyimides modified with poly(butylene terephthalate) reported previously in the literature.[51,52] For elongation at break, it can be observed that the values recorded for polyimides with naphthalene units in the diamine segment are higher than those for polyimides that contain methylene bridge in the diamine segment, except for **PI-6** which shows value comparable to those of **PI-1** to **PI-5**. This result can be explained probably by the presence of ether linkages in both or only in one segment, diamine and dianhydride, which introduces a higher flexibility in the main chain leading to the increase of the elongation at break.

The Young's moduli of polyimide films are in the range 1706–2375 MPa. These results are comparable with the data reported for unmodified polyimides[51] and for polyimides modified with silica tubes[53] or with mesoporous silica.[54]

The morphology of polyimide films is an important parameter which influences membrane properties. Therefore, the surface morphology of these films, as-deposited on glass plates, was investigated using AFM in semi-contact mode. Table 4 presents the root mean square roughness of all polyimide films. Figure 7 shows two-dimensional and three-dimensional height images and cross-section profiles, taken along the straight lines in the two-dimensional images, which were obtained for polyimide films of **PI-1** and **PI-2**. The AFM examination of the films reveals homogeneous and compact surfaces without any phase separation, with a very good quality, without peaks or pinholes. An interesting observation can be made when comparing the surface roughness data for the MMDA- and BAPN-based series. From the lower root mean square roughness values for the MMDA-based polyimides than for the analogous polyimides obtained from BAPN, i.e. **PI-8** and **PI-4**, **PI-7** and **PI-2**, and **PI-6** and **PI-1**, it appears that polyimide films derived from MMDA display much smoother surfaces.

These observations are consistent with $T_g$ differences, found to be around 20 °C, between the respective members of both series, where MMDA-based polyimides, due to the smaller number of flexible ether linkages, exhibit more rigid structures. It may therefore be a reasonable supposition that, when comparing similar polyimide structures, it will be those of a more flexible nature that will be more able to form surfaces with greater roughness.

## Gas permeation properties

Gas permeation results for the polyimide films prepared in this work are given in Table 5. The observed order of permeability



  

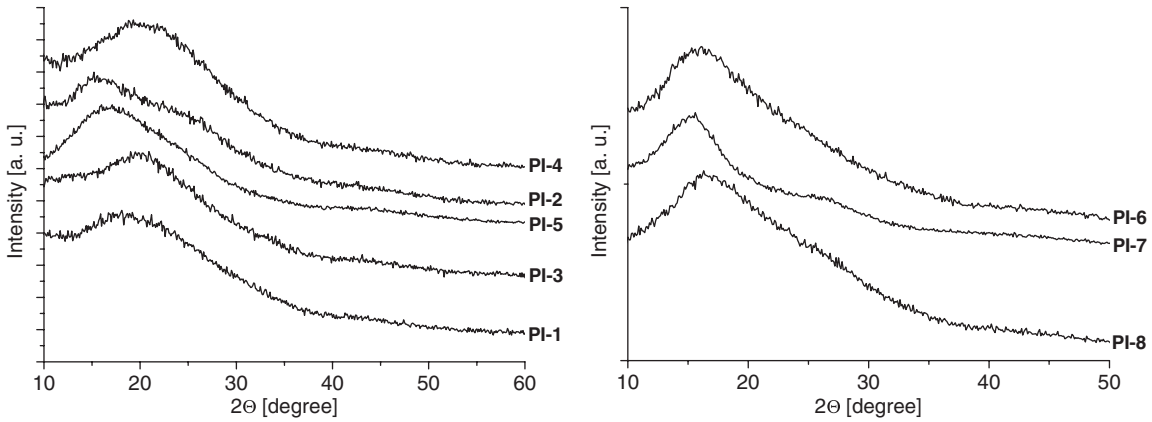


**Figure 4.** Wide-angle XRD patterns of the polyimide films.

**Table 3.** Thermal characteristics and *d*-spacing values of the polyimide films

| Polymer | *d*-spacing (Å) | $T_5$[a] (°C) | $T_{max}$[b] (°C) | Char yield[c] (%) | $T_g$[d] (°C) |
|---|---|---|---|---|---|
| **PI-1** | 4.76 | 505 | 540 | 60 | 208 |
| **PI-2** | 5.68 | 525 | 550; 615 | 61 | 264 |
| **PI-3** | 4.55 | 520 | 575 | 65 | 256 |
| **PI-4** | 4.35 | 525 | 580 | 62 | 252 |
| **PI-5** | 5.24 | 525 | 550; 610 | 63 | 211 |
| **PI-6** | 5.57 | 475 | 515 | 60 | 226 |
| **PI-7** | 5.75 | 495 | 546; 630 | 60 | 286 |
| **PI-8** | 5.37 | 498 | 550 | 66 | 273 |

[a] Temperatures of 5% weight loss.
[b] Temperature of maximum decomposition rate.
[c] Residual weight when heated at 800 °C in nitrogen.
[d] Estimated using DSC during the second run. Similar TGA and DSC results for **PI-6**, **PI-7** and **PI-8** to those obtained here can be found elsewhere.[31]

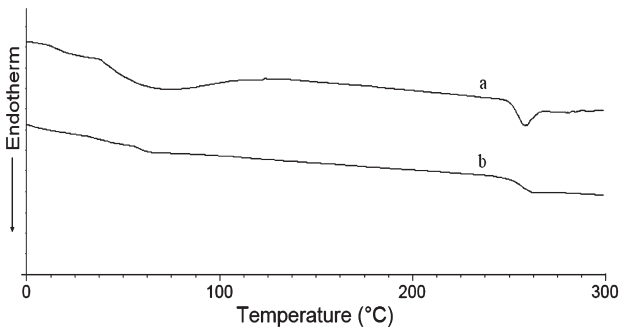


**Figure 5.** DSC curves of **PI-2** obtained at a heating rate of 20 °C min$^{-1}$: (a) first heating run; (b) second heating run after cooling at 20 °C min$^{-1}$.

for the tested gases is as follows: He > $CO_2$ > $O_2$ > $N_2$, which is the order of their increasing kinetic diameter, and is in accordance with other results found in the literature concerning gas permeation in glassy polymers.[22] As can be seen from the permeability data, **PI-7**, containing hexafluoroisopropylidene moieties in the main chain along with methyl substituents on the benzene ring, exhibits both highest gas permeability and selectivity.

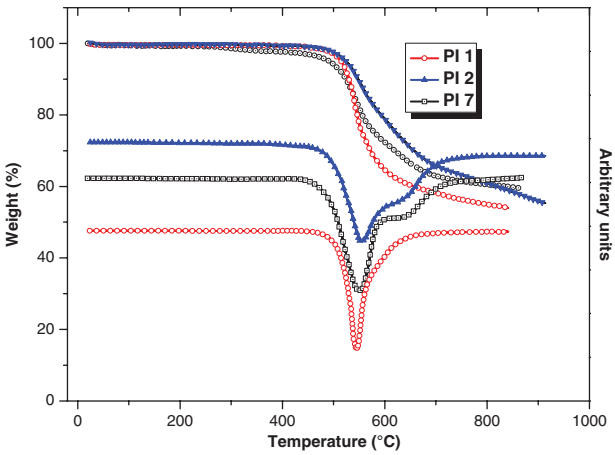


**Figure 6.** TGA curves of **PI-1**, **PI-2** and **PI-7**.

**Table 4.** Mechanical properties and surface roughness parameters of polyimide films

| Polymer | Tensile strength (MPa) | Elongation at break[a] (%) | Young's modulus (MPa) | RMS[b] (nm) |
|---|---|---|---|---|
| **PI-1** | 88 | 8.5 | 1946 | 0.72 |
| **PI-2** | 64 | 6.5 | 1706 | 1.18 |
| **PI-3** | 70 | 5.1 | 2036 | 1.71 |
| **PI-4**[c] | – | – | – | 0.56 |
| **PI-5** | 85 | 8.8 | 2375 | 1.88 |
| **PI-6** | 91 | 8.2 | 2020 | 0.35 |
| **PI-7** | 60 | 3.2 | 1750 | 0.68 |
| **PI-8** | 77 | 4.1 | 2010 | 0.35 |

[a] Initial slope of the stress–strain curve.
[b] Root mean square roughness.
[c] Broken during testing.

This is consistent with the highest *d*-spacing and $T_g$ values determined for this polymer. Furthermore, the permeability of **PI-2** synthesized using BAPN and **IIb** is found to be lower than that of **PI-7** obtained from MMDA and the same **IIb**, and much higher than those of the other synthesized polyimides. The permeation property of **PI-2** is again in accordance with its *d*-spacing and

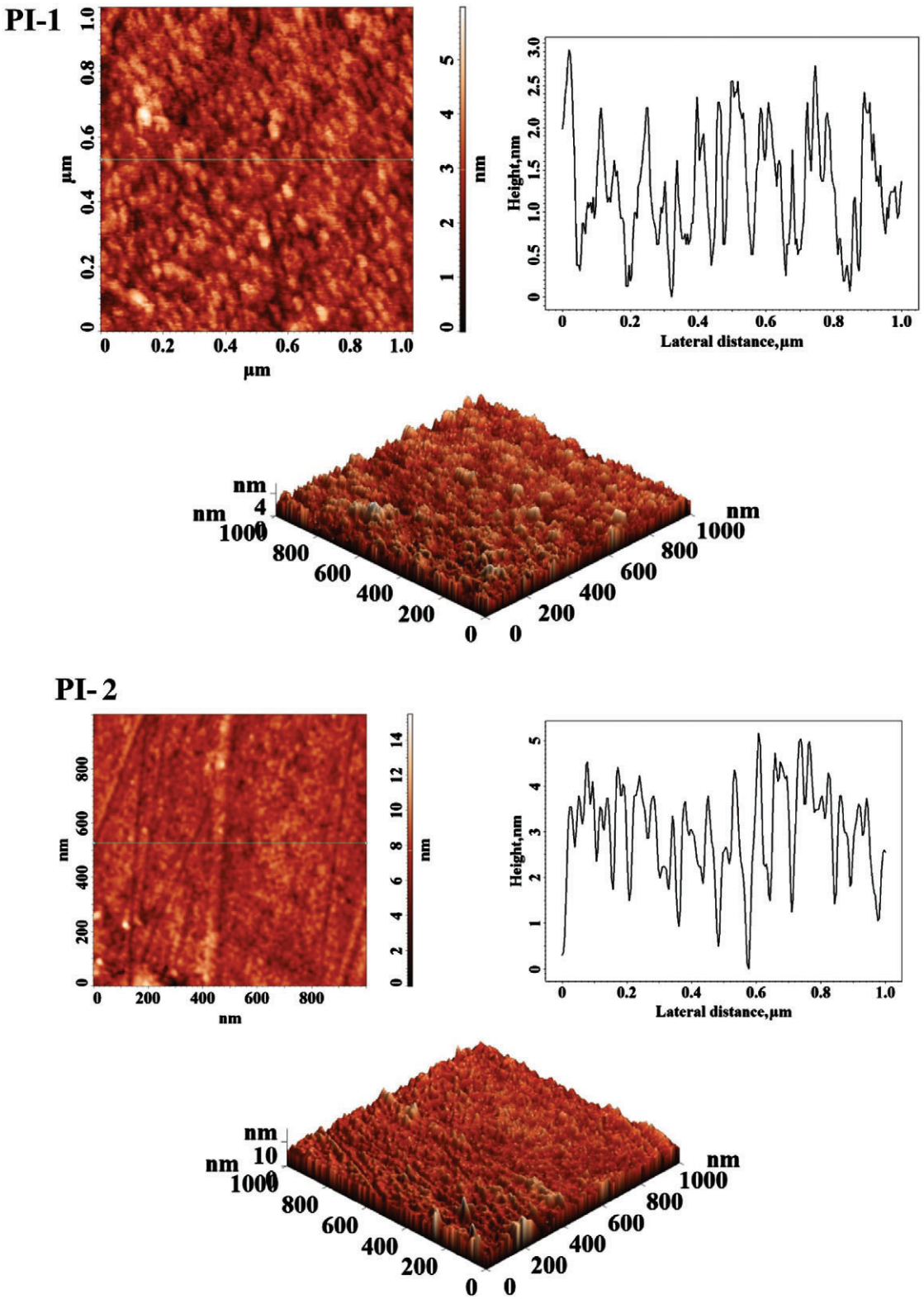


**Figure 7.** AFM images of **PI-1** and **PI-2** films.

$T_g$ values, which both rank it as second among the polyimides studied. The *d*-spacing and $T_g$ parameters are commonly correlated with the ability of a given polymer matrix for permeation of small molecules. Generally, the larger the interchain spacing, the lower is the chain packing density and the higher is the gas permeability. Often, permeability is well correlated with fractional free volume (FFV), as suggested from theoretical considerations,[55] which is used as a tool for structure characterization. It is well known that the presence of $CF_3$ groups produces larger and more effective free volume elements for gas diffusion, and also supplies



  

**Table 5.** Gas permeation properties of the polyimide films at 30 °C

| Polymer | Permeability, *P* (Barrer) | | | | Selectivity, $\alpha$ | |
|---|---|---|---|---|---|---|
| | $N_2$ | $O_2$ | He | $CO_2$ | $O_2/N_2$ | $CO_2/N_2$ |
| **PI-1** | 0.065 | 0.374 | 8.50 | 1.085 | 5.7 | 16.7 |
| **PI-2** | 0.168 | 0.918 | 15.86 | 3.351 | 5.5 | 19.9 |
| **PI-3** | 0.096 | 0.536 | 12.48 | 1.650 | 5.6 | 17.2 |
| **PI-4** | 0.019 | 0.109 | 4.74 | 0.337 | 5.7 | 17.7 |
| **PI-5** | 0.105 | 0.616 | 14.40 | 1.620 | 5.9 | 15.4 |
| **PI-6** | 0.080 | 0.468 | 10.47 | 1.254 | 5.8 | 15.7 |
| **PI-7** | 0.249 | 1.680 | 50.41 | 6.810 | 6.7 | 27.3 |
| **PI-8** | 0.019 | 0.136 | 7.68 | 0.587 | 7.2 | 30.9 |

more sites for gas sorption, both factors contributing to higher permeability.[56] However, the permeability data obtained for **PI-2** and **PI-5** demonstrate that this general trend may be upset, and the effectiveness of $CF_3$ groups in increasing permeability may be reduced if the chain stiffness is significantly decreased as indicated by the lower $T_g$ value of **PI-5**. Comparing the permeability data of **PI-3** and **PI-1**, it can also be noticed that the asymmetric bulky fluorene group at the aliphatic carbon atom introduces more FFV into the polymer matrix than it does the isopropylidene one. This result correlates with the higher $T_g$ value of **PI-3** than **PI-1**, and conforms to the reports that FFV in some glassy polymers increases with an increase of $T_g$ as a result of increasing chain stiffness. Replacement of hexafluoroisopropylidene groups by isopropylidene ones is known to reduce gas permeability,[20,50] and the results obtained in this work for **PI-5** and **PI-1** confirm this observation. Moreover, they are in accordance with the relative structural differences between these two polymers, i.e. with lower *d*-spacing and slightly lower $T_g$ values of **PI-1** compared to those of **PI-5**. The lowest gas permeability is observed for **PI-4** and **PI-8**, which are both based on dianhydride containing carbonyl linkage. This is due to the polarity of carbonyl groups, which provides high interaction among the polymer chains leading to high packing density of the respective polymers. Generally, high chain stiffness, as indicated by the high $T_g$ values, is expected to result in relatively high selectivity, and the same tendency can be observed in this work. Among the polyimides studied, **PI-7** and **PI-8**, both showing the highest $T_g$ values, are also found to be the most selective ones. When comparing both polymers with their analogues from the BAPN series, it can easily be seen that replacement of MMDA with BAPN, which is sterically less bulkier and incorporates flexibility into the polymer chain through ether linkages, significantly decreases selectivity of the respective polyimides, compare **PI-4** with **PI-8** and **PI-2** with **PI-7**. All the experimental data obtained imply that chain mobility and interchain distance are closely related to the gas permeation ability when structurally similar polyimides are compared. However, they are not the only factors controlling gas permeation, and their usefulness in drawing more general relationships between structure and permeation properties is limited. This is in accordance with our earlier conclusions[57] and with other literature data.[58–60]

## CONCLUSIONS

Aromatic polyimides were prepared from BAPN or MMDA and different aromatic dianhydrides. These polymers were soluble in many organic solvents, and showed high glass transition temperature, and excellent thermal stability. The thin films cast from solutions of these polyimides were optically transparent, and exhibited good mechanical properties. AFM investigations revealed that these films had homogeneous and compact surfaces with low surface roughness values. XRD of the polyimide films showed diffused patterns indicating the amorphous nature of these polymers. The presence of a hexafluoroisopropylidene group in the dianhydride segments along with methyl substituents in the diamine ones led to the highest gas permeation rates through the polyimide films. However, the material separation characteristics for $O_2/N_2$ and $CO_2/N_2$ gas pairs appeared to be below the respective upper bounds.

## ACKNOWLEDGEMENT

The research leading to these results has received funding from the European Union's Seventh Framework Program (FP7/2007-2013) under grant agreement no. 264115-STREAM.

## REFERENCES

1 Maier G, *Prog Polym Sci* **26**:3–65 (2001).
2 Volksen W, Miller RD and Dubois G, *Chem Rev* **110**:56–110 (2010).
3 McKeown NB and Budd PM, *Macromolecules* **43**:5163–5176 (2010).
4 Dhara MG and Banerjee S, *Prog Polym Sci* **35**:1022–1077 (2010).
5 Ritter N, Senkovska I, Kaskel S and Weber J, *Macromolecules* **44**:2025–2033 (2011).
6 Liaw D-J, Wang K-L, Huang Y-C, Lee K-R, Lai J-Y and Ha C-S, *Prog Polym Sci* **37**:907–974 (2012).
7 Liu Y-L, Wang K-L, Huang G-S, Zhu C-X, Tok E-S, Neoh K-G *et al.*, *Chem Mater* **21**:3391–3399 (2009).
8 Chavez R, Ionescu E, Fasel C and Riedel R, *Chem Mater* **22**:3823–3825 (2010).
9 Farha OK, Bae Y-S, Hauser BG, Spokoyny AM, Snurr RQ, Mirkin CA *et al.*, *Chem Commun* **46**:1056–1058 (2010).
10 Weber J, Schmidt J, Thomas A and Bohlmann W, *Langmuir* **26**:15650–15656 (2010).
11 Rao KV, Haldar R, Kulkarni C, Maji TK and George SJ, *Chem Mater* **24**:969–971 (2012).
12 Ritter N, Antonietti M, Thomas A, Senkovska I, Kaskel S and Weber J, *Macromolecules* **42**:8017–8020 (2009).
13 Sava I, Chisca S, Bruma M and Lisa G, *Polym Bull* **65**:363–375 (2010).
14 Sydlik SA, Chen Z and Swager TM, *Macromolecules* **44**:976–980 (2011).
15 Chisca S, Sava I and Bruma M, *Polym Int* **62**:1634–1643 (2013).
16 Chen JC, Wu JA, Chang HW and Lee CY, *Polym Int* **63**:352–362 (2014).
17 Cecopieri-Gomez ML, Palacios-Alquisira J and Dominguez JM, *J Membr Sci* **293**:53–65 (2007).
18 Xiao Y, Low BT, Hosseini SS, Chung TS and Paul DR, *Prog Polym Sci* **34**:561–580 (2009).
19 Calle M, Lozano AE, de la Campa JG and de Abajo J, *Macromolecules* **43**:2268–2275 (2010).
20 Dasgupta B and Banerjee S, *J Membr Sci* **362**:58–67 (2010).
21 Maya EM, Garcia-Yoldi I, Lozano AE, de la Campa JG and de Abajo J, *Macromolecules* **44**:2780–2790 (2011).
22 Cho YJ and Park HB, *Macromol Rapid Commun* **32**:579–568 (2011).
23 Ghanem BS, McKeown NB, Budd PM, Selbie JD and Fritsch D, *Adv Mater* **20**:2766–2771 (2008).
24 Ghanem BS, McKeown NB, Budd PM, Al-Harbi NM, Fritsch D, Heinrich K *et al.*, *Macromolecules* **42**:7881–7888 (2009).
25 Ma X, Swaidan R, Belmabkhout Y, Zhu Y, Litwiller E, Jouiad M *et al.*, *Macromolecules* **45**:3841–3849 (2012).
26 Ma X, Salinas O, Litwiller E and Pinnau I, *Macromolecules* **46**:9618–9624 (2013).
27 Soo CY, Jo HJ, Lee YM, Quay JR and Murphy MK, *J Membr Sci* **444**:365–377 (2013).
28 Guo R, Sanders DF, Smith ZP, Freeman BD, Paul DR and McGrath JE, *J Mater Chem A* **1**:262–272 (2013).
29 Robeson LM, *J Membr Sci* **320**:390–400 (2008).
30 Yang C-P, Hsiao S-H and Chung C-L, *Polym Int* **54**:716–724 (2005).
31 Chisca S, Sava I, Musteata VE and Bruma M, *Eur Polym J* **47**:1186–1197 (2011).
32 Han X, Tian Y, Wang L, Xiao C and Liu B, *Eur Polym J* **43**:4382–4388 (2007).

  

33 Leu TS and Wang CS, *Polymer* **43**:7069–7074 (2002).
34 Sava I, *Mater Plast* **43**:15–19 (2006).
35 Schwartz WT, *High Perform Polym* **2**:189–196 (1990).
36 Hsiao SH and Li CT, *J Polym Sci A: Polym Chem* **37**:1403–1412 (1999).
37 Chisca S, Barzic AI, Sava I, Olaru N and Bruma M, *J Phys Chem B* **116**:9082–9088 (2012).
38 Wolińska-Grabczyk A, Jankowski A, Sekuła R and Kruczek B, *Sep Sci Technol* **45**:1231–1240 (2011).
39 Sava I, Chisca S, Bruma M and Lisa G, *J Therm Anal Calorim* **104**:1135–1143 (2011).
40 Sava I and Chisca S, *Mater Chem Phys* **134**:116–121 (2012).
41 Ando S, Matsuura T and Sasaki S, *Polym J* **29**:69–76 (1997).
42 Choi MC, Hwang JC, Kim C, Ando S and Ha CS, *J Polym Sci A: Polym Chem* **48**:1806–1814 (2010).
43 Guo YZ, Shen DX, Ni HJ, Liu JG and Yang SY, *Prog Org Coat* **76**:768–777 (2013).
44 Zhai L, Yang S, and Fan L, *Polymer* **53**:3529–3539 (2012).
45 Kazama S, Teramoto T and Haraya K, *J Membr Sci* **207**:91–104 (2002).
46 Velioglu S, Ahunbay MG and Tantekin-Ersolmaz SB, *J Membr Sci* **417–418**:217–227 (2012).
47 Shimazu A, Miyazaki T and Ikeda K, *J Membr Sci* **166**:113–118 (2000).
48 Grabiec E, Schab-Balcerzak E, Wolinska-Grabczyk A, Jankowski A, Jarzabek B, Kozuch-Krawczyk J *et al.*, *Polym J* **43**:621–629 (2011).
49 Ronova IA and Bruma M, *Struct Chem* **23**:47–54 (2012).
50 Dasgupta B, Sen SK and Banerjee S, *J Membr Sci* **345**:249–256 (2009).
51 Bruma M, Damaceanu MD and Muller P, *High Perform Polym* **21**:522–534 (2009).
52 Zabaleta A, González I, Eguiazábal JI and Nazábal J, *Eur Polym J* **45**:466–473 (2009).
53 Zhang Y, Li Y, Li G, Huang H, Chan HLW, Daoud WA *et al.*, *Chem Mater* **19**:1939–1945 (2007).
54 Lin J and Wang X, *Polymer* **48**:318–329 (2007).
55 Pixton MR and Paul DR, Relationships between structure and transport properties for polymers with aromatic backbones, in *Polymeric Gas Separation Membranes*, ed. by Paul DR, Yampolskii YuP. CRC Press, Boca Raton, FL, pp. 83–154 (1994).
56 Chang KS, Hsiung CC, Lin CC and Tung KL, *J Phys Chem B* **113**:10159–10169 (2009).
57 Wolinska-Grabczyk A, Schab-Balcerzak E, Grabiec E, Jankowski A, Matlengiewicz M, Szeluga U *et al.*, *Polym J* **45**:1202–1209 (2013).
58 Hirayama Y, Yoshinaga T, Kusuki Y, Ninomiya K, Sakakibara T and Tamari T, *J Membr Sci* **111**:169–182 (1996).
59 Sanders DF, Smith ZP, Guo R, Robeson LM, McGrath JE, Paul DR *et al.*, *Polymer* **54**:4729–4761 (2013).
60 Koley T, Bandyopadhyay P, Mohanty AK and Banerjee S, *Eur Polym J* **49**:4212–4223 (2013).




  